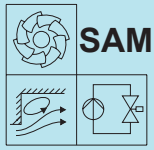




TECHNISCHE UNIVERSITÄT  
KAISERSLAUTERN

Lehrstuhl für  
Strömungsmechanik und  
Strömungsmaschinen - SAM



Hrsg. Prof. Dr.-Ing. M. Böhle

# SAM - Fortschrittsberichte

**Band 21**

Thomas Reviol

**A design process for propellers  
for the agitation of high viscous  
fluids based on the design  
analysis of wind turbine blades**

# **A design process for propellers for the agitation of high viscous fluids based on the design analysis of wind turbine blades**

Vom Fachbereich Maschinenbau und Verfahrenstechnik  
der Technischen Universität Kaiserslautern  
zur Erlangung der venia legendi für das Fach

**Fluid mechanics and energy technology**

genehmigte Habilitationsschrift

von  
Herrn

**Dr.-Ing. Thomas Reviol**  
aus Saarbrücken

D386

Dekan: Prof. Dr.-Ing. Tilmann Beck  
Gutachter: Prof. Dr.-Ing. Martin Böhle  
Prof. Dr.-Ing. habil. Uwe Janoske

Tag der Einreichung: 06.10.2020  
Tag des Habilitationsvortrags: 29.06.2021



SAM-Fortschrittsberichte

Band 21

**Thomas Reviol**

**A design process for propellers for the agitation of  
high viscous fluids based on the design analysis  
of wind turbine blades**

D 386 (Habil.-Schr. Technische Universität Kaiserslautern)

Shaker Verlag  
Düren 2021

**Bibliographic information published by the Deutsche Nationalbibliothek**

The Deutsche Nationalbibliothek lists this publication in the Deutsche Nationalbibliografie; detailed bibliographic data are available in the Internet at <http://dnb.d-nb.de>.

Zugl.: Kaiserslautern, TU, Habil.-Schr.,

Copyright Shaker Verlag 2021

All rights reserved. No part of this publication may be reproduced, stored in a retrieval system, or transmitted, in any form or by any means, electronic, mechanical, photocopying, recording or otherwise, without the prior permission of the publishers.

Printed in Germany.

ISBN 978-3-8440-8188-6

ISSN 2191-8031

Shaker Verlag GmbH • Am Langen Graben 15a • 52353 Düren

Phone: 0049/2421/99011-0 • Telefax: 0049/2421/99011-9

Internet: [www.shaker.de](http://www.shaker.de) • e-mail: [info@shaker.de](mailto:info@shaker.de)

to my father



# Acknowledgements

An undertaking such as this can never be accomplished without the help and support of others. In recent years, I have enjoyed the support of many friends and colleagues in the completion of this work. It is not possible to thank everyone who supported me here. I would like to thank everyone who has supported me and I would like to pay special tribute to a select few who played a significant or special part in the completion of this work:

First of all, I would like to thank Prof. Dr.-Ing. Martin Böhle for his many years of support and for our numerous professional and critical discussions. In addition to Prof. Dr.-Ing. Martin Böhle, I also want to thank Prof. Dr.-Ing. Uwe Janoske for preparing the expert reports. I would also like to express my thanks to the members of the Habilitation Commission: Prof. Dr.-Ing. Martin Böhle, Prof. Dr. Nicolas Gauger, Prof. Dr.-Ing. Erik von Harbou, Prof. Dr.-Ing. Alois Schlarb, Dr.-Ing. Kai Nikolaus and Janik Röckel.

I would also like to thank all my colleagues who I have worked with at the Institute over the years for their good cooperation and mutual support. In particular, Stefan Kluck and Peng Wang, with whom I had the opportunity to conduct some joint research.

Over the years, some colleagues became friends. To name a few of them: Rebecca Schäfer, Marco Schönwald and Anika Theis. They were always prepared to lend me a sympathetic ear. Especially the many supportive discussions with Anika Theis gave me further motivation, particularly towards the final stages of my thesis, which helped me to complete the thesis.

Most of all, I would like to thank my family: my wife Rebecca and my three children Lillie, Nora and Erik. Over the years, my family have experienced many highs and lows and has always accepted these in a wonderful way. They supported and motivated me every step of the way. Without them, this thesis would never have been possible. Thank you so much!

Obersülzen, July 2021, Thomas Reviol









# Abstract

The subject of this thesis is the design of axial flow machines. The type of turbomachine under examination is used to supply energy for high viscous fluid flow, as used in mixing and stirring tasks. The high viscous media treated in these tasks usually have non-Newtonian fluid properties. This kind of fluid flow is frequently associated with the field of energy and process engineering. In order to narrow down the problem described, the field of turbomachinery is restricted to the consideration of propellers. Propellers are used in a wide range of fluid mechanics tasks. In the form of wind turbines, propellers extract kinetic energy from a control room and thereby slow down the flow. Propeller stirrers, on the other hand, increase the energy level of a flow and accelerate it. Both machines are based on the same principle – only the direction of the energy flow is to be considered as the opposite direction.

The design of new agitators is usually based on experience. Often, agitators are, therefore, not flow-optimised, and cannot be optimally operated. In this thesis, it is investigated whether the design processes of modern wind turbines, which are considered to be mature, can be adapted in order to generate a flow-optimised geometry for this type of turbomachine as well.

This thesis will first examine the basics of wind turbine design processes. Special attention will be paid to the differences caused by the viscous fluid properties under consideration. The highly viscous behaviour of the fluids under consideration means that the theoretical fundamentals have to be extended as a result. Such extensions are identified and supplement the theoretical basis. The thesis will then present and examine an analytically based design process for flow-optimised propeller mixers. The procedure is based on *blade element momentum theory*.

Application of *blade element momentum theory* requires detailed knowledge of the aerodynamic behaviour of the profiles used. This behaviour is usually only known for low viscosity and high-Re applications, as is usually the case for wind turbines or propeller engines. Comprehensive profile characteristics are not available for highly viscous and low-Re applications. In this thesis, these basics are generated using numerical methods.

In the next step, the newly introduced design method is combined with the results of the investigations of profile aerodynamics for high viscous low-Re fluid flow. This combination is done using a calculation process which produces the flow-optimised geometry of a propeller mixer. The theoretical principles of the methods are implemented in an algorithm in such a way that the resultant turbomachine can be designed for a previously selected operating point, the design point. In contrast to classical turbomachinery, the design point additionally requires the specification of viscous fluid properties. However, in practical use, the final selected operating point of a turbomachine is often not the design point. The algorithm is examined for its suitability for inverse power calculation as well in order to compute the complete characteristic curve for a previously generated propeller mixer already in the design process.

# Kurzfassung

Die vorliegende Arbeit stellt einen Beitrag zur Auslegung axial fördernder Strömungsmaschinen dar. Der untersuchte Typ einer Strömungsmaschine dient der Energiezufuhr in Strömungen hochviskoser Medien, wie diese z.B. für Misch- und Rühraufgaben eingesetzt werden. Die dort behandelten hochviskosen Medien verfügen meist über nichtnewtonsche Fluideigenschaften und treten häufig im Bereich der Energie- und Verfahrenstechnik auf.

Um das beschriebene Problem einzugrenzen, steht als Strömungsmaschine der Propeller im Fokus der Arbeit. Propeller werden in vielfältigen strömungsmechanischen Fragestellungen eingesetzt. In Form von Windenergieanlagen entziehen Propeller einem Kontrollraum kinetische Energie, und verzögern auf diese Art die Strömung. Propellerrührer hingegen erhöhen das Energieniveau einer Strömung und beschleunigen diese. Beide Maschinen basieren auf denselben Grundlagen – lediglich die Richtung des Energieflusses ist entgegengesetzt zu betrachten.

Der Entwurf neuer Rührorgane basiert in der Regel auf Erfahrung. Oft verfügen Rührorgane deswegen nicht über eine strömungsoptimierte Form und können nicht optimal betrieben werden. In dieser Arbeit wird untersucht, ob die als ausgereift geltende Auslegungsprozedur moderner Windenergieanlagen auf Propellerrührer adaptiert werden kann, um eine strömungsoptimierte Geometrie auch für diese Art Strömungsmaschine zu generieren.

Zunächst werden in dieser Arbeit die Grundlagen der Auslegungsprozeduren von Windenergieanlagen analysiert. Insbesondere die Unterschiede infolge des betrachteten Fluides werden hierbei berücksichtigt. Durch das hochviskose Verhalten der betrachteten Fluide ergeben sich notwendige Erweiterungen der theoretischen Grundlagen. Diese werden identifiziert und die theoretische Basis wird um diese notwendigen Erweiterungen ergänzt. Daran anschließend wird eine analytisch basierte Auslegungsprozedur für strömungsoptimierte Propellermischer eingeführt und untersucht. Diese basiert auf der Verwendung der *Blattelement-Momenten-Methode*.

Die Verwendung der *Blattelement-Momenten-Methode* erfordert das detaillierte Wissen über das aerodynamische Verhalten der eingesetzten Profile.

Dieses Verhalten ist bislang meist nur für niedrigviskose high-Re Anwendungsfälle bekannt, wie dies üblicherweise bei Windenergieanlagen oder bei Propellertriebwerken der Fall ist. Für hochviskose low-Re Anwendungen sind umfassende Profilcharakteristika nicht vorhanden. Diese Grundlagen werden im Rahmen dieser Arbeit mit numerischen Methoden generiert.

Die neu eingeführte Auslegungsprozedur wird im letzten Schritt der Arbeit mit der Profilaerodynamik für hochviskose low-Re Strömungen kombiniert. Die Kombination erfolgt in einer numerischen Prozedur, deren Resultat die strömungsoptimierte Geometrie eines Propellerrührers ist. Die theoretischen Grundlagen der Methoden werden derart in einem Algorithmus umgesetzt, dass die resultierende Strömungsmaschine für einen zuvor gewählten Auslegungspunkt zur Verfügung gestellt werden kann. Im Gegensatz zum klassischen Strömungsmaschinenbau erfordert der Auslegungspunkt zusätzlich die Angabe der viskosen Fluideigenschaften.

Kenntnisse über den im Betrieb anfallenden Leistungsbedarf einer Strömungsmaschine sind wesentlich zur Einsparung von Ressourcen. Häufig ist der gewählte Betriebspunkt einer Strömungsmaschine allerdings nicht der Auslegungspunkt. Es wird daher weiterhin untersucht, inwiefern der verwendete Algorithmus invers ausgeführt werden kann, um das Leistungskennfeld a priori für zuvor generierte Propeller zu berechnen.







# Contents

<b>List of Figures</b>	<b>x</b>
<b>List of Tables</b>	<b>xi</b>
<b>Nomenclature</b>	<b>xii</b>
<b>I. Synopsis</b>	<b>1</b>
<b>1. Introduction</b>	<b>3</b>
1.1. Subject of research . . . . .	3
1.2. Objective . . . . .	4
1.3. Solution concept . . . . .	5
1.3.1. Overview . . . . .	6
1.3.2. Problems to solve . . . . .	7
<b>2. Brief literature overview</b>	<b>11</b>
2.1. Mixer design processes . . . . .	11
2.2. Wind turbines . . . . .	18
<b>II. Fundamentals</b>	<b>25</b>
<b>3. Fluid mechanics of flow profiles</b>	<b>27</b>
3.1. Profile aerodynamics . . . . .	27
3.1.1. General description . . . . .	28
3.2. Blade element momentum theory . . . . .	34
3.2.1. Axial momentum theory . . . . .	35
3.2.2. Blade element theory . . . . .	43
<b>4. Wind turbine design methods</b>	<b>48</b>
4.1. Principles of wind turbines . . . . .	48

4.2. Momentum method . . . . .	50
4.2.1. Betz-Joukowsky maximum . . . . .	50
4.2.2. Optimum blade dimension . . . . .	53
4.2.3. Rotational wake enhancement . . . . .	59
4.2.4. Further losses . . . . .	64
4.2.5. Final design process . . . . .	65
4.3. Vortex methods . . . . .	67
<b>5. High viscous fluid flow</b>	<b>73</b>
5.1. Flow of matter . . . . .	73
5.1.1. Ideal constitutive laws . . . . .	73
5.1.2. General fluid flow . . . . .	77
5.1.3. Introduction of generalised Newtonian fluid flow . . . . .	80
5.2. Generalised Newtonian fluids . . . . .	81
5.2.1. Phenomenology . . . . .	81
5.2.2. State of deformation . . . . .	84
5.2.3. State of stress . . . . .	87
5.2.4. Reiner-Rivlin constitutive law . . . . .	89
5.2.5. Empirical laws . . . . .	92
5.3. Similarity mechanics . . . . .	97
5.3.1. Introduction to Buckingham's theorem . . . . .	98
5.3.2. Common Reynolds number calculation . . . . .	101
5.3.3. Rheological adjusted Reynolds number . . . . .	102
<b>6. Introduction to jet theory</b>	<b>109</b>
6.1. General theory . . . . .	110
6.2. Jet theory for propeller propulsion . . . . .	112
6.2.1. Introducing the assumptions . . . . .	112
6.2.2. Universal law of propeller jets . . . . .	114
6.2.3. Semi-empirical law of propeller jets . . . . .	117
6.2.4. Jet theory for non-Newtonian fluid flow . . . . .	121

---

<b>III. Method development and validation</b>	<b>125</b>
<b>7. Method development</b>	<b>127</b>
7.1. Analytical approach . . . . .	127
7.1.1. Kinematic conditions in a jet . . . . .	127
7.1.2. Loads caused by the flow . . . . .	139
7.1.3. Derivation of the propeller shape . . . . .	141
7.2. Underlying polar plot database . . . . .	144
7.2.1. Selected profiles . . . . .	144
7.2.2. Numerical setup . . . . .	145
7.2.3. Validation study . . . . .	150
7.2.4. Results of the database . . . . .	159
7.3. Developed algorithm . . . . .	162
7.3.1. Design point calculation . . . . .	162
7.3.2. Inverse calculation of characteristics . . . . .	167
<b>8. Application of the method</b>	<b>174</b>
8.1. Deriving the geometrical shape . . . . .	174
8.1.1. Propeller A . . . . .	175
8.1.2. Propeller B . . . . .	179
8.2. Predicting characteristics . . . . .	185
8.2.1. Propeller A . . . . .	185
8.2.2. Propeller B . . . . .	188
<b>9. Experimental investigations</b>	<b>191</b>
9.1. Model fluid study . . . . .	191
9.2. Test configuration . . . . .	196
9.2.1. Propeller A . . . . .	197
9.2.2. Propeller B . . . . .	201
9.3. Preliminary investigations . . . . .	208
9.3.1. Propeller A . . . . .	209
9.3.2. Propeller B . . . . .	210
9.3.3. Assessment of the model assumptions . . . . .	213

9.4. Supplementary investigations . . . . .	214
9.4.1. Measurement methodology . . . . .	214
9.4.2. Jet distribution . . . . .	216
<b>IV. Discussion and review of the method</b>	<b>227</b>
<b>10. Discussion of the method</b>	<b>229</b>
10.1. Disadvantages of the method . . . . .	229
10.1.1. Limited application range . . . . .	229
10.1.2. Polar plot database . . . . .	230
10.1.3. Influence of the Reynolds number . . . . .	231
10.1.4. Influence of modelling assumptions . . . . .	233
10.2. Discussion of the measurements . . . . .	235
<b>11. Conclusion and outlook</b>	<b>237</b>
11.1. Conclusion . . . . .	237
11.2. Outlook . . . . .	239
<b>Bibliography</b>	<b>255</b>
<b>Appendix</b>	<b>258</b>
<b>A. Measurement devices</b>	<b>259</b>
A.1. Viscometer . . . . .	259
A.2. Torque sensors . . . . .	263
A.3. Ultrasonic Doppler anemometry . . . . .	265
A.3.1. Technical specifications . . . . .	265
A.3.2. Technical drawings . . . . .	272
<b>B. Drive devices</b>	<b>273</b>
B.1. DC-motors . . . . .	273
B.2. Hydraulic motor . . . . .	275

B.3. Bearings . . . . .	277
B.3.1. Radial bearing . . . . .	277
B.3.2. Axial bearing . . . . .	279
<b>C. Model fluid</b>	<b>281</b>
C.1. Xanthan gum . . . . .	281
C.2. Carboxymethyl cellulose . . . . .	282
<b>D. Historic figures</b>	<b>283</b>
<b>E. Results</b>	<b>285</b>
E.1. Polar plot database . . . . .	285
E.2. Jet distribution . . . . .	288
E.2.1. True-to-scale velocity . . . . .	288
E.2.2. Normalised velocity . . . . .	297
E.2.3. Similarly scaled velocity . . . . .	306

## List of Figures

2.1	Historical application of mixers . . . . .	12
2.2	Historical results of power characteristics . . . . .	14
2.3	Mixer types . . . . .	17
2.4	The Persian windmill . . . . .	19
2.5	V164-9.5 MW turbines from MHI Vestas Offshore Wind . . . . .	22
3.1	Geometrical description of a profile . . . . .	29
3.2	Aerodynamic loads on a profile under flow conditions . . . . .	30
3.3	Distribution of the pressure coefficient over a profile . . . . .	31
3.4	Aerodynamic characteristics of a profile . . . . .	33
3.5	Lilienthal polar of a profile . . . . .	34
3.6	Elementary stream tube . . . . .	37
3.7	Momentum balance . . . . .	40
3.8	Infinitesimal blade element . . . . .	43
3.9	Velocity triangle and forces . . . . .	45
4.1	Wind energy principles . . . . .	49
4.2	Course of ideal power coefficient over velocity ratio . . . . .	53
4.3	Circumferential forces at radial section . . . . .	55
4.4	Chord length and relative angle for ideal blade design . . . . .	57
4.5	Stream tube around swirl-affected fluid machine . . . . .	60
4.6	Velocity triangle and forces, considering circulation . . . . .	61
4.7	Chord length and relative angle according to Schmitz . . . . .	63
4.8	Typical blade with multiple airfoil profiles . . . . .	66
4.9	Single-blade, detailed view of hub and tip . . . . .	67
4.10	Vortices for rotating propellers . . . . .	68
4.11	Circulation and vortex filament, around airfoil . . . . .	69
4.12	Circulation vortex filament for elliptic distribution . . . . .	70
5.1	Newton's law . . . . .	74
5.2	Hooke's law . . . . .	75
5.3	Maxwell model . . . . .	77

---

5.4	Pipkin's diagram . . . . .	78
5.5	Classification of matter . . . . .	80
5.6	Purely viscous and time independent fluids . . . . .	82
5.7	Flow characteristics of a shear-thinning fluid . . . . .	83
5.8	Deformation of a fluid element . . . . .	85
5.9	State of stress of a fluid element . . . . .	88
5.10	Relevant quantities of a mixing process . . . . .	98
5.11	Differences in Reynolds number definitions . . . . .	104
5.12	Relevant quantities at an airfoil . . . . .	105
6.1	Definition sketch of plane turbulent jets . . . . .	110
6.2	Dimensionless velocity distribution of a plane jet . . . . .	111
6.3	Schematic view of a propeller jet . . . . .	115
6.4	Change in the maximum velocity of a propeller jet . . . . .	119
6.5	Calculation of the velocity distribution in a propeller jet . . . . .	121
6.6	Comparison of experiment with jet theory . . . . .	122
7.1	Sectional view of a propeller jet . . . . .	128
7.2	Mass flow rates in the jet . . . . .	129
7.3	Stream tube to derive the axial momentum theory . . . . .	133
7.4	Velocity triangles at the propeller . . . . .	139
7.5	Loads at a radial section . . . . .	140
7.6	Normalised plot of the three preselected flow profiles . . . . .	145
7.7	Schematic view of the fluid domain . . . . .	147
7.8	Computational grid for the LB-method . . . . .	149
7.9	Computational grid for the RANS-method . . . . .	152
7.10	Flow field around E817 profile: velocity . . . . .	154
7.11	Flow field around E817 profile: static pressure . . . . .	155
7.12	Flow field around E817 profile: dynamic viscosity . . . . .	156
7.13	Flow field around E817 profile: velocity and viscosity . . . . .	157
7.14	Profile polar plots of the validation study . . . . .	158
7.15	Resulting profile polar data . . . . .	160
7.16	Flow chart for the design of a propeller mixer . . . . .	163



## List of Figures

---

7.17	Flow chart for the inverse calculation . . . . .	169
8.1	Propeller A, chord length, angle, and polar data . . . . .	177
8.2	Propeller A, point cloud of the shape . . . . .	178
8.3	Propeller A, different views . . . . .	179
8.4	Propeller A, manufactured prototype . . . . .	180
8.5	Propeller B, chord length, angle, and polar data . . . . .	181
8.6	Propeller B, point cloud of the shape . . . . .	182
8.7	Propeller B, different views . . . . .	183
8.8	Propeller B, manufactured prototype . . . . .	184
8.9	Calculated characteristics of Propeller A . . . . .	187
8.10	Calculated characteristics of Propeller B . . . . .	188
9.1	Viscosity of different model fluids . . . . .	192
9.2	Viscoelastic characteristics of different model fluids . . . . .	193
9.3	Additives used to produce the applied model fluids . . . . .	195
9.4	Test stand for Propeller A . . . . .	197
9.5	Model fluid of Propeller A . . . . .	199
9.6	Geometrical overview of the test basin for Propeller B . . . . .	202
9.7	Test setup for Propeller B, schematics . . . . .	203
9.8	Test setup for Propeller B, photography . . . . .	204
9.9	UDA sensor, technical sheet . . . . .	204
9.10	Model fluid of Propeller B . . . . .	207
9.11	Experimental data of Propeller A, torque over speed . . . . .	210
9.12	Experimental data of Propeller B, torque over speed . . . . .	212
9.13	Data acquisition points . . . . .	215
9.14	Measurement result C1-N100, normalised . . . . .	219
9.15	Measurement result C2-N100, normalised . . . . .	222
9.16	Measurement result C3-N100, normalised . . . . .	224
A.1	Excerpt of viscometer tech. spec., page 7 . . . . .	259
A.2	Excerpt of viscometer tech. spec., page 52 . . . . .	260
A.3	Excerpt of viscometer tech. spec., page 53 . . . . .	261
A.4	Excerpt of viscometer tech. spec., page 55 . . . . .	262

---

A.5	Excerpt of torque sensor tech. spec., page 1 . . . . .	263
A.6	Excerpt of torque sensor tech. spec., page 2 . . . . .	264
A.7	Excerpt of UDA sensor tech. spec., page 1 . . . . .	265
A.8	Excerpt of UDA sensor tech. spec., page 2 . . . . .	266
A.9	Excerpt of UDA sensor tech. spec., page 3 . . . . .	267
A.10	Excerpt of UDA sensor tech. spec., page 4 . . . . .	268
A.11	Excerpt of UDA sensor tech. spec., page 5 . . . . .	269
A.12	Excerpt of UDA sensor tech. spec., page 6 . . . . .	270
A.13	Excerpt of UDA sensor tech. spec., page 7 . . . . .	271
A.14	Technical drawings of the UDA sensor . . . . .	272
B.1	Technical specifications of DC-motor Size 1 . . . . .	273
B.2	Technical specifications of DC-motor Size 2 . . . . .	274
B.3	Excerpt of hydraulic motor tech. spec., page 25 . . . . .	275
B.4	Excerpt of hydraulic motor tech. spec., page 29 . . . . .	276
B.5	Tech. spec. of radial air bearing, dimensions . . . . .	277
B.6	Tech. spec. of radial air bearing, performance data . . . . .	277
B.7	Technical drawings of radial air bearing . . . . .	278
B.8	Axial air bearing tech. spec., dimensions . . . . .	279
B.9	Axial air bearing tech. spec., performance data . . . . .	279
B.10	Technical drawings of axial air bearing . . . . .	280
C.1	Technical specifications of XG . . . . .	281
C.2	Technical specifications of CMC . . . . .	282
D.1	Historic illustration of sections of a stork's wing . . . . .	283
D.2	Historic illustration of a polar curve of a flat plate . . . . .	283
D.3	Historic patent, investigated profile forms . . . . .	284
E.1	Profile polar data for profile E817 . . . . .	285
E.2	Profile polar data for profile NLF1015 . . . . .	286
E.3	Profile polar data for profile FX60-126 . . . . .	287
E.4	Measurement result C1-N085 . . . . .	288
E.5	Measurement result C1-N100 . . . . .	289

---

## List of Figures

---

E.6	Measurement result C1-N115 . . . . .	290
E.7	Measurement result C2-N085 . . . . .	291
E.8	Measurement result C1-N100 . . . . .	292
E.9	Measurement result C2-N115 . . . . .	293
E.10	Measurement result C3-N085 . . . . .	294
E.11	Measurement result C3-N100 . . . . .	295
E.12	Measurement result C3-N105 . . . . .	296
E.13	Measurement result C1-N085, normalised . . . . .	297
E.14	Measurement result C1-N100, normalised . . . . .	298
E.15	Measurement result C1-N115, normalised . . . . .	299
E.16	Measurement result C2-N085, normalised . . . . .	300
E.17	Measurement result C2-N100, normalised . . . . .	301
E.18	Measurement result C2-N115, normalised . . . . .	302
E.19	Measurement result C3-N085, normalised . . . . .	303
E.20	Measurement result C3-N100, normalised . . . . .	304
E.21	Measurement result C3-N105, normalised . . . . .	305
E.22	Measurement result C1-N085, similarly scaled . . . . .	306
E.23	Measurement result C1-N100, similarly scaled . . . . .	307
E.24	Measurement result C1-N115, similarly scaled . . . . .	308
E.25	Measurement result C2-N085, similarly scaled . . . . .	309
E.26	Measurement result C2-N100, similarly scaled . . . . .	310
E.27	Measurement result C2-N115, similarly scaled . . . . .	311
E.28	Measurement result C3-N085, similarly scaled . . . . .	312
E.29	Measurement result C3-N100, similarly scaled . . . . .	313
E.30	Measurement result C3-N105, similarly scaled . . . . .	314

---

## List of Tables

5.1. Parameter range of Herschel and Bulkley regression . . . . .	95
5.2. Laws to model pure viscous fluid flow . . . . .	97
7.1. Parameters of the investigated flow profiles . . . . .	146
7.2. Boundary and solver conditions for LBM and RANS . . . . .	151
7.3. Required input parameters for design point calculation . . . . .	164
7.4. Required input parameters for inverse calculation . . . . .	170
8.1. Calculated process parameters of Propeller A . . . . .	176
8.2. Calculated process parameters of Propeller B . . . . .	184
8.3. Operating point and design parameters of Propeller A . . . . .	186
8.4. Operating point and design parameters of Propeller B . . . . .	189
9.1. Rheological parameters, Propeller A . . . . .	201
9.2. Rheological parameters, design fluid, Propeller B . . . . .	206
9.3. Rheological parameters, operating fluids, Propeller B . . . . .	208
9.4. Measurement plan of Propeller B . . . . .	211
9.5. Measurement results of Propeller B . . . . .	213
9.6. Operating points of the detailed investigations . . . . .	218

# Nomenclature

## Latin symbols

Symbol	Description	Unit
<b>1</b>	Unit tensor	—
<i>a</i>	Factor of interference, approximation factor	—
<i>A</i>	Area	$m^2$
<i>b</i>	Width	$m$
<i>c</i>	Absolute velocity	$m/s$
<i>c</i>	Concentration	$wt.\%$
<i>C</i>	Coefficient	—
<i>D</i>	Diameter	$m$
<b>D</b>	Rate of deformation tensor	$s^{-1}$
<i>De</i>	Deborah number	—
<i>E</i>	Energy	$J$
<i>f</i>	Function	—
<i>F</i>	Force	$N$
<i>F</i>	Antiderivative of a function	—
<i>g</i>	Gravity constant	$m s^{-2}$
<i>G</i>	Shear modulus	$MPa$
<i>H</i>	Height	$m$
<i>i</i>	Control variable	—
<i>I</i>	Momentum	$N s$
<i>j</i>	Control variable	—
<i>k</i>	Control variable	—
$\kappa$	Consistency	$Pa s^m$
<i>l</i>	Chord length	$m$
<i>L</i>	Length	$m$
<b>L</b>	Velocity gradient tensor	$s^{-1}$
<i>m</i>	Mass	$kg$
<i>m</i>	Flow index	—

---

<b>Symbol</b>	<b>Description</b>	<b>Unit</b>
$\dot{m}$	Mass flow rate	$kg\ s^{-1}$
$\vec{n}$	Normal vector	$m$
$n$	Shaft speed	$min^{-1}$
$n_z$	Amount of an entity	–
$Ne$	Newton number	–
$p$	Pressure	$Pa$
$P$	Power	$W$
$R$	Radius	$m$
$r$	Coordinate, radial direction	$m$
$Re$	Reynolds number	–
<b>S</b>	Cauchy stress tensor	$Pa$
$t$	Time	$s$
$T$	Torque	$Nm$
<b>T</b>	Extra stress tensor	$Pa$
$\mathcal{T}$	Mixing time	$s$
$u$	Circumferential velocity	$m/s$
$v$	Velocity magnitude	$m/s$
$v_x$	Velocity component in x-direction	$m/s$
$v_y$	Velocity component in y-direction	$m/s$
$v_z$	Velocity component in z-direction	$m/s$
$V$	Volume	$m^3$
$\dot{V}$	Volume flow rate	$l\ s^{-1}$
$w$	Relative velocity	$m/s$
$x$	Coordinate, x-direction	$m$
$\mathfrak{X}$	Arbitrary entity	[...]
$\underline{\mathfrak{X}}$	Matrix with arbitrary entities	[...]
$y$	Coordinate, y-direction	$m$
$z$	Coordinate, z-direction	$m$

## Greek symbols

Symbol	Description	Unit
$\alpha$	Flow angle	$^{\circ}$
$\gamma$	Shear strain	—
$\dot{\gamma}$	Rate of shear strain	$s^{-1}$
$\Gamma$	Circulation	$m^2 s^{-1}$
$\delta$	Glide angle	$^{\circ}$
$\varepsilon$	Longitudinal strain	—
$\epsilon$	Lift-to-drag ratio	—
$\dot{\epsilon}$	Rate of longitudinal strain	$s^{-1}$
$\zeta$	Angle of jet divergence	$^{\circ}$
$\eta$	Efficiency	—
$\theta$	Temperature	$K$
$\vartheta$	Coordinate, angular direction	$^{\circ}$
$\Theta$	Relative angle	$^{\circ}$
$\lambda$	Relaxation time	$s$
$\Lambda$	Tip speed ratio	—
$\mu$	Dynamic viscosity	$Pa s$
$\mu_0$	Dynamic zero-shear-rate-viscosity	$Pa s$
$\mu_{\infty}$	Dynamic infinity-shear-rate-viscosity	$Pa s$
$\nu$	Kinematic viscosity	$m^2 s^{-1}$
$\pi$	Dimensionless entity, Archimedes' constant	—
$\rho$	Density	$kg m^{-3}$
$\sigma$	Normal stress	$Pa$
$\varsigma$	Standard deviation	[...]
$\tau$	Shear stress	$Pa$
$\tau_0$	Yield stress	$Pa$
$\Upsilon$	Auxiliary function	[...]
$\varphi$	Mounting angle	$^{\circ}$
$\chi$	Scalar-valued function	[...]
$\psi$	Normal stress coefficient	$Pa s^2$
$\omega$	Frequency	$s^{-1}$

## Subscripts

Symbol	Description
0	Point upstream from propeller
1	Point in propeller plane
2	Point downstream from propeller
$-\infty$	Unaffected position, upstream from propeller
$+\infty$	Unaffected position, downstream from propeller
$\infty$	Ambient condition
C	Circumferential
CA	Profile camber
Co	Entity of core or initial region of jets
D	Drag
Dev	Entity of fully developed flow of jets
Des	Design point
Eff	Effective value
En	Entrainment
L	Lift
Hub	Hub
Ind	Induced
Jet	Jet
LE	Leading edge
m	Meridional component
max	Maximum value
mean	Mean value
n	Normal component of an entity
OP	Operating point
P	Quantity related to propeller
PP	Quantity related to the propulsion
R	Resulting
t	Tangential component of an entity
T	Thrust
TE	Trailing edge



## Nomenclature

---

<b>Symbol</b>	<b>Description</b>
TH	Profile thickness
u	Swirl component

---

## Superscripts

Symbol	Description
$x^*$	Hypothetical value
$\vec{x}$	Vectorial formulation of an entity
$\bar{x}$	Mean value
$\hat{x}$	Arbitrary spatial position
$\check{x}$	Reaction force
$\tilde{x}$	Simplified value
$x'$	Space derivative
$\dot{x}$	Time derivative
$x^+$	Dimensionless distance in space
$x_{\mathcal{P}-}$	Entity infinitesimal upstream from point $\mathcal{P}$
$x_{\mathcal{P}+}$	Entity infinitesimal downstream from point $\mathcal{P}$

## Abbreviations

Symbol	Description
<i>BEM</i>	Blade element momentum theory
<i>CAD</i>	Computer aided design
<i>CMC</i>	Carboxymethyl cellulose
<i>CFD</i>	Computational fluid dynamics
<i>GG</i>	Guar gum
<i>LBM</i>	Lattice-Boltzmann method
<i>LES</i>	Large eddy simulation
<i>LVE</i>	Linear viscoelastic regime
<i>NLVE</i>	Non-linear viscoelastic regime
<i>PAA</i>	Polyacrylamide
<i>RANS</i>	Reynolds-averaged Navier-Stokes equations
<i>UDA</i>	Ultrasonic Doppler anemometry
<i>XG</i>	Xanthan gum